

X International Conference on Structural Dynamics, EURODYN 2017

# Aerodynamic properties of Wind Turbine Towers based on Wind Tunnel Experiments

Robert Fontecha<sup>a</sup>, Bettina Henneke<sup>a</sup>, Frank Kemper<sup>a</sup>, Markus Feldmann<sup>b</sup> \*

<sup>a</sup>Center for Wind and Earthquake Engineering, RWTH Aachen University, Mies-van-der-Rohe-Str. 1, Aachen 52074, Germany

<sup>b</sup>Institute of Steel Construction, RWTH Aachen University, Mies-van-der-Rohe-Str. 1, Aachen 52074, Germany

---

## Abstract

The presented investigations aim to suggest more realistic models to predict the dynamic behavior of wind turbine structures. Two key issues are addressed: the aerodynamic damping and the cross-wind vibrations.

Based on experimental studies in the boundary layer wind tunnel, aerodynamic information for both effects has been obtained. A scaled model of a wind energy tower (1:150) in combination with complementary models have been tested in a test bench designed to carry out HFFB, dynamic wind pressure and forced-oscillation experiments. Reynolds number based scale effects on the tower model have been studied previously.

In the predictions of cross-wind vibrations, the length related correlation of vortices shedding from cylindrical structures plays an important role. Therefore, wind dynamic pressures were measured along static tower and cylinder models using pressure taps to determine realistic values of the vortex shedding correlation length.

Motion-induced wind vibrations can be significantly influenced by the aerodynamic damping. Using the forced-oscillations method, experiments have been performed under controlled system oscillation with varying wind speed in prism models and tower model. The measured base model forces were correlated with the model motion using spectral methods to obtain the corresponding aerodynamic stiffness and damping coefficients.

Both aerodynamic studies will allow more detailed models for the design of new wind tower structures. The acquired information will be applicable in MB-simulations to obtain more realistic and accurate wind turbine performances

© 2017 The Authors. Published by Elsevier Ltd.

Peer-review under responsibility of the organizing committee of EURODYN 2017.

---

\* Robert Fontecha. Tel.: +49-241-8026238; fax: +49-241-8022140.

E-mail address: [fontecha@cwe.rwth-aachen.de](mailto:fontecha@cwe.rwth-aachen.de)

**Keywords:** Aerodynamic Damping; Vortex-shedding correlation length; Wind turbine towers; Aeroelasticity

## 1. Introduction

For the design of wind turbine towers, a realistic prediction of the overall structural dynamic behavior is still an important issue as it is influenced by various dynamic interactions. As the costs for the tower structure amounts about 15-25% of the whole investment, it is of interest to avoid unnecessary over-safeties. The presented investigations aim to suggest more realistic models to predict the dynamic behavior of wind turbine structures. Two key issues are addressed: the aerodynamic damping and the cross-wind vibrations.

## 2. Wind tunnel and test bench

All measurements were carried out in the Boundary Layer Wind Tunnel (BLWT) of the Institute of Steel constructions of the RWTH Aachen. In this first phase of the study, the measurements of the different models were done under wind speed and turbulence profiles similar to a terrain category II according to EC1 [1] (see Fig. 1). These profiles are better simulated in their lower parts, which is a common phenomenon in BLWT. In future studies, special focus will be set on the higher profile parts, which affect the wind turbine rotor.

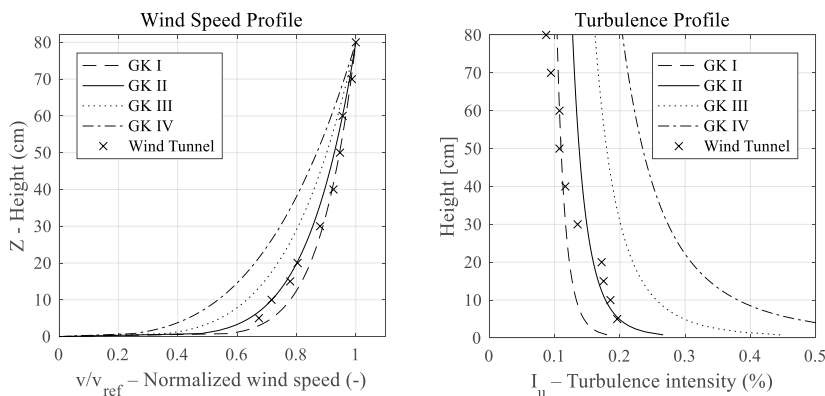


Fig. 1. Wind speed and Turbulence profiles in the BLWT during measurements.

Following the HFFB approach (see [2, 3]), the test bench was designed to be stiff enough as to not affect the base balance measurements at the frequency range of interest. At the same time, it was equipped with a mixture of slider-crank and scotch yoke mechanisms in combination with a three-phase motor with adjustable rotation speed to carry out forced, sinusoidal oscillation. The base forces and moments were measured through a six-axis balance sensor. Accelerations and dynamic pressures on the models were measured synchronously to the base forces in most tests. More detailed information about the test bench can be found in Henneke [4].

## 3. Scale effects on wind turbine tower modelling

When modelling round sections for wind tunnel tests, scale effects due to different Reynolds numbers in full-scale prototype and small-scale model can change the flow characteristics around the studied model. Previous studies regarding scale effects on the tower model were carried out. The used geometric scale coefficient  $\lambda_g=1:150$  was chosen to avoid blockage according to the used wind tunnel section.

Considering the definition of the Reynolds number  $Re=b \cdot u/v$ , with  $b$  the cylinder diameter,  $u$  the incoming wind speed and  $v$  the air kinematic viscosity, it is clear that a reduction of the tower model diameter  $b$  due to geometrical scaling requires an equal increase of the wind speed  $u$  if same Reynolds numbers are pursued (dynamic similarity, see

[5], [6]), which is not achievable in most cases. An alternative approach considerably studied in the past ([7–10]), is surface roughness modification. In this case, the objective is to force a premature transition of the flow to a turbulent boundary layer, achieving in the otherwise subcritical flow regime of the model a similar flow behavior as in the prototype's transcritical flow regime, which corresponds to Reynolds numbers around  $Re=10^6$  and above.

Several surface modifications based on existing literature were applied to PMMA cylinders with dimensions  $L \times D = 750 \times 30 \text{ mm}$ . The models surfaces were smooth, with indented patterns as in Hojo [5, 6], dimpled patterns as in Bearman and Harvey [7], and different sandpapers classified as in FEPA P. The flow regime present in the tests was determined through force coefficient and chordwise dynamic pressure measurements. All tests were done with close to laminar inflow conditions. The influence of turbulence will be studied and quantified in future measurements.

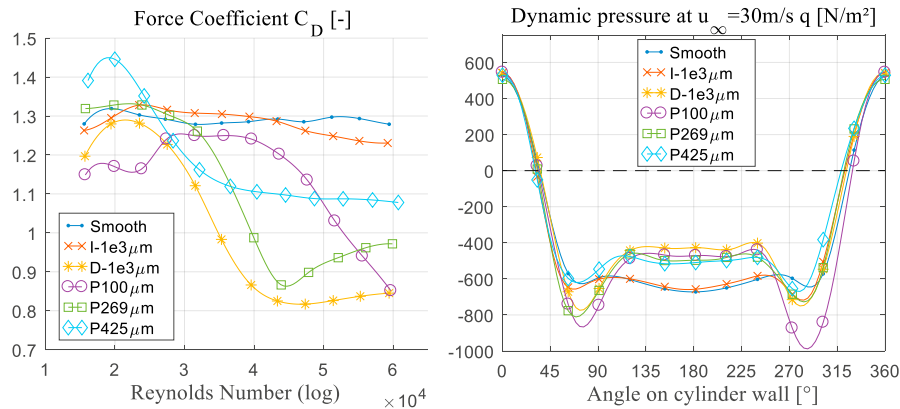


Fig. 2. Drag force coefficients vs. Reynolds Number(left) and chordwise dynamic pressures at  $u_\infty=30\text{m/s}$  of tested cylinders

The results in Fig. 2 show that supercritical to transcritical flow regimes can be achieved through surface roughness modification at much lower wind speeds than those required for smooth cylinders. However, the required high wind speeds would prevent setting realistic tip speed ratios and thus the aerodynamic similarity of wind turbine models in future experiments. Therefore, the following tests were done with a smooth tower model in subcritical flow regime. The impact of scale effects on aerodynamic damping and correlation length will be studied in additional future experiments.

The used tower model corresponds to a tower prototype with 112m height (the hub height being 115m), taper ratio of 0.02 and first eigenfrequency of about 0.5 Hz. Applying the scale factor  $\lambda_g=1:150$  results in a tower model height of about 750mm

#### 4. Vortex shedding correlation length

##### 4.1. The correlation Length

Vortex-induced vibrations can cause considerable tower fatigue damage during the tower construction process and wind turbine standstill. The number of relevant parameters affecting vortex shedding vibrations is high and often not free from uncertainty. In this section, only the vortex-shedding correlation length will be studied in more detail.

The correlation length is a way of expressing a length along the structure in which vortex-shedding occurs synchronously to some degree, and therefore favoring sinusoidal loading of the structure. Assuming a cylindrical structure, the spatial, normalized cross-correlation coefficient  $\rho_{1,2}$  of the wind dynamic pressures is calculated between the reference point  $p_1$  and a point  $p_2$ , which varies along the structure height. This procedure results in the spatial, spanwise correlation  $\rho_{1,x}$ , which can be understood as a curve of correlation coefficients between points  $p_1$  and  $p_x$  (see [8–10]). As these curves are often not completely defined within the model length, they were fitted through exponential mathematical expressions of the form  $\rho_{1,x}(r) = e^{-cr}$ , with  $r$  the coordinate along the cylinder axis (see more

details in Novak and Tanaka [10]). The area under this curve can be calculated and expressed as the area of a rectangle with height 1 and length the correlation length  $L^*$ , which is usually normalized with the cylinder diameter  $d$ .

#### 4.2. Correlation length measurements

A static wind tunnel test (without model oscillation) was carried out with a PMMA cylinder of 50mm constant diameter. The measuring points were located at  $90^\circ$  respect to the wind attack angle and separated 50mm in spanwise direction. The reference wind speeds ranged between 5 and 17.5 m/s in the measurements. Next figure shows the used model in the BLWT (see Fig.3, left), together with a visualization of the determined correlation lengths along the cylinder height for  $v_{\text{ref}}=15\text{m/s}$ . The correlation length values in the model middle sector declined slightly with increasing wind speed, being the values at 17.5m/s approx. 10% smaller than at 10m/s. The progression of the values with the height matches the expected values: the correlation lengths are smaller in the lower model sector, where the wind speed profile is steeper, and in the extreme upper sector, where tip effects become important (see Fig.3, right).

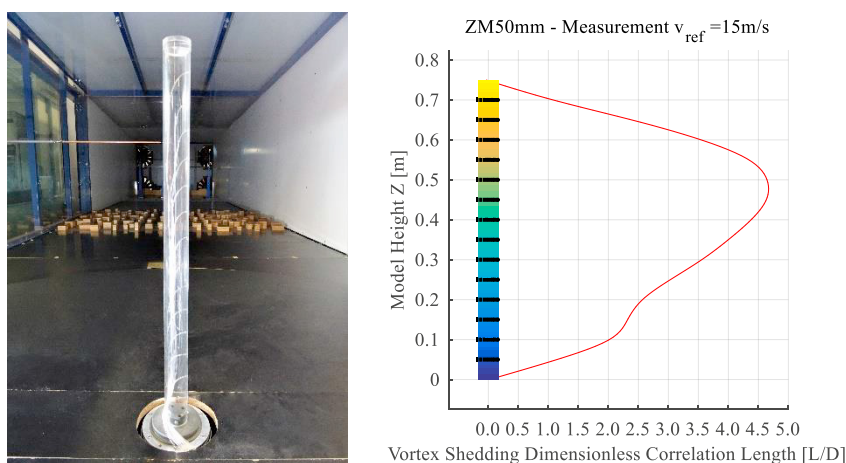


Fig.3. PMMA cylinder model (left) and dimensionless correlation length along cylinder height (right)

Table 1 shows the mean values of the dimensionless correlation length in the studied wind speed range.

Table 1. Averaged dimensionless correlation length  $L^*/d$  [-] along cylinder height  $H$  [m].

H [m]	0.05	0.10	0.15	0.20	0.25	0.30	0.35	0.40	0.45	0.50	0.55	0.60	0.65	0.70
$L^*/d$ [-]	1.06	2.31	2.29	2.59	3.10	3.69	4.16	4.47	4.68	4.71	4.45	3.64	2.47	0.89

First static measurements on the wind turbine tower model of section 3 showed no correlation. This was attributed to the high separation of the pressure taps (125mm) and to fast varying vortex shedding frequencies along the tower model due to its taper ratio. Future measurements will study the influence on the correlation length of taper ratio, terrain category and turbulence in static measurements, as well as oscillation amplitude and frequency.

## 5. Aerodynamic damping

### 5.1. Across-wind oscillations: Measurement analysis

The theoretic background and formulation of the aerodynamic stiffness and damping are mainly based on the work of Steckley [11], the acquisition of the motion-dependent wind forces from the measurements are based on the work of Hortmanns [12] and on previous studies [13].

The wind forces due to the model motion are expressed through a complex aerodynamic impedance as in Steckley [11]. It is composed of a component proportional to the displacement, i.e. the real part or aerodynamic stiffness  $\alpha$ , and a component proportional to the motion speed, i.e. the imaginary part or aerodynamic damping  $\beta$ . When forcing a cylinder model to oscillate in a sinusoidal, pivoting mode, this wind forces can be expressed as:

$$M(t) = \frac{1}{6} \rho_a \pi D^2 H^2 \omega^2 \hat{Y} (\alpha \cos(\omega t) + \beta \sin(\omega t)) \quad (1)$$

Where  $\rho_a$  is the air density,  $D$  the model diameter,  $H$  the model height,  $\omega$  the angular frequency and  $\hat{Y}$  the oscillation amplitude. A more detailed derivation of these forces can be found in [11]. Spectral methods were used for the separation of the aerodynamic forces (see [12] and [13]). The base moments and accelerations were measured synchronously during the wind tunnel tests and correlated with each other to obtain the aerodynamic force components. This can be visualized in the following figure:

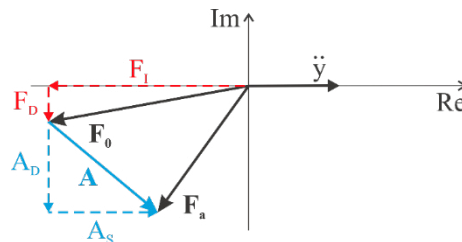


Fig. 4: Identification of the aerodynamic forces in the complex plane

The acceleration  $\ddot{y}$  determines the orientation of the real axis. In tests without wind action, the sum of forces  $F_0$  is measured, and the inertial and structural damping forces  $F_I$  and  $F_D$  are determined by separating real from imaginary part in the integral of the cross-spectrum between  $\ddot{y}$  and  $F_0$ . In tests with wind action,  $F_a$  is measured, and knowing  $F_0$ , the aerodynamic stiffness and damping  $A_s$  and  $A_D$  can be determined. Details on this matter can be found in [13].

## 5.2. Results of measurement of the aerodynamic coefficients

The methodology in section 5.1 was firstly applied to prism models with ratios  $H/B=6.67$  and tip oscillation amplitudes  $y/B=4.82\%$  under an oncoming wind as described in section 2. The results were compared with similar experiments from Steckley [11] with a good agreement between both results, as it can be seen in Fig. 5:

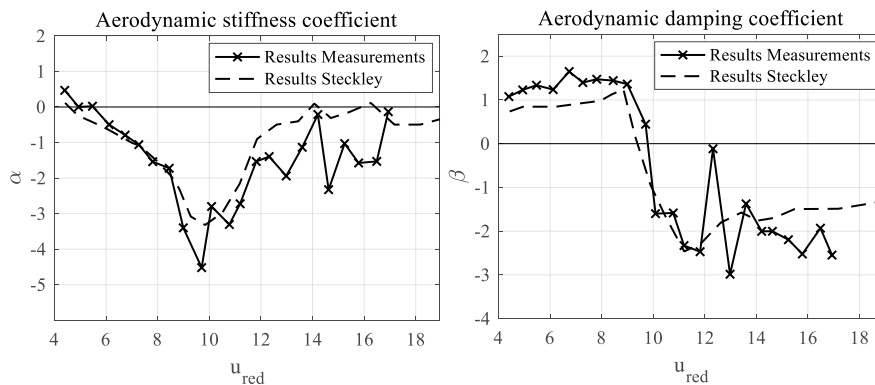


Fig. 5: Comparison of aerodynamic stiffness and damping coefficients with the results of Steckley [11]

More details about the used models, experiments and measurement evaluation can be found in Henneke [4].

Measurements in the tower model failed to measure aerodynamic forces due to its reduced dimensions. Therefore, the measurements will be done in the future with larger cylinder models.

## 6. Summary

The experiments exposed in this paper establish the foundations for following measuring campaigns to determine vortex-shedding correlation lengths and aerodynamic structure coefficients of wind turbines and their support towers.

The determined correlation lengths on a cylinder model under terrain category II according to EC1 [1] constitutes a good basis to following planned research on factors affecting it, such as terrain category, turbulence, taper ratio, and oscillation amplitude in future dynamic tests. The first measurements on the tower model already show the potentially high impact of those factors (in this case the taper ratio).

The aerodynamic coefficients determined on prism models confirm the validity of the used test bench and spectral methods. Following validations with existing international benchmarks for the HFFB method, as well as measurements on cylinder-like structures are planned for a near future.

As scale effects affect the flow characteristics substantially, additional experiments will be required to study the impact of flow regime changes on the measured magnitudes.

## Acknowledgements

The results exposed hereby are extracted of the BMWI-project BBTI-WEA with funding code 0325793. The project is funded by the German Federal Ministry of Economics and Energy (BMWI) according to a decision of the German Federal Parliament. The authors of this paper cordially thank for the funding of this project.

## References

- [1] 2010. "Eurocode 1: Actions on structures - Part 1-4: General actions - Wind actions, No. BS EN 1991-1-4:2005+A1:2010 (Apr. 2010).
- [2] Boggs, D. W. and Peterka, J. A. "Aerodynamic Model Tests of Tall Buildings. *Journal of Engineering Mechanics* 115, No. 3, pp. 618–635, 1989.
- [3] Tschanz, T. and Davenport, A. G. "The base balance technique for the determination of dynamic wind loads. *Journal of Wind Engineering and Industrial Aerodynamics* 13, No. 1-3, pp. 429–439, 1983.
- [4] Henneke, B. "Automatisierte Bestimmung der Windeinwirkung auf hohe Bauwerke durch Windkanalversuche mit der "High Frequency Force Balance"-Methode und der Methode der erzwungenen Schwingungen. Master Thesis, RWTH, 2017.
- [5] Hojo, T., 2015. "Control of flow around a circular cylinder using a patterned surface. In CMEM 2015. WIT Transactions on Modelling and Simulation. WIT PressSouthampton, UK, pp. 245–256. DOI=10.2495/CMEM150221.
- [6] Tetsuo Hojo, Shinsuke YAMAZAKI, Hiroyuki OKADA. "Development of lowdrag aerodynamically stable cable with indented processing. Special Issue on Steel Structure No.82. Nippon Steel Technical Report, 2000.
- [7] BEARMAN, P. W. and HARVEY, J. K. "Control of circular cylinder flow by the use of dimples. *AIAA Journal* 31, No. 10, pp. 1753–1756, 1993.
- [8] Ruscheweyh, H. "Dynamische Windwirkung an Bauwerken. "1. Grundlagen. Anwendungen 1. Bauverl., Wiesbaden, Berlin, 1982.
- [9] Ruscheweyh, H. "Dynamische Windwirkung an Bauwerken. "2. Praktische Anwendungen 2. Bauverl., Wiesbaden, Berlin, 1982.
- [10] Novak, M. and Tanaka, H., 1977. "Pressure correlations in a vibrating cylinder. In *Proceedings of the Fourth International Conference on Wind Effects on Buildings and Structures*, Heathrow, 1975, K. J. Eaton, Ed. Cambridge University Press, Cambridge [England], New York, pp. 227–232.
- [11] Steckley, A. "Motion-induced wind forces on chimneys and tall buildings. Canadian theses = Thèses canadiennes. National Library of Canada, Ottawa, 1990.
- [12] Hortmanns, M. "Zur Identifikation und Berücksichtigung nichtlinearer aeroelastischer Effekte. *Stahlbau* H. 34. Shaker, Aachen, 1997.
- [13] Fontecha, R. "Determination of flutter derivatives of bridge sections Determination of flutter derivatives of bridge sections based on wind tunnel experiments under forced excitation. Master Thesis, UPC/RWTH Aachen, 2012.